Microbubble generation using a syringe pump.

Cyrille Lenders, Michaël Gauthier, Pierre Lambert

Microbubble Generation Using a Syringe Pump

Cyrille Lenders, Michaël Gauthier and Pierre Lambert[‡]

November 3, 2009

Abstract

The context of this paper is to study the use of capillary microgripper in submerged mediums which requires the use of microbubbles. This paper presents a model and experimentations of the generation of bubbles. In the microsystems which uses liquid, gas bubbles can generate forces due to the surface tension at their interface. To use these bubbles, it is necessary to generate them in a controlled way. In this paper, we propose to study the generation of a bubble having a defined volume, using a syringe pump based device. We first build a mathematical model to predict the growth of the bubble in the liquid. Indeed, the compressibility of the gas and the effect of surface tension are of major importance at microscale, and our model will demonstrate the existence of an instability during the bubble growth. We proceed with a dimensionless study that will allow to predict the existence of the instability on the basis of a dimensionless number. Finally, we present experimental results to validate the mathematical model.

1 Introduction

The study of micromanipulations consists in producing methods able to position objects whose size is typically from 1 µm to 1 mm. Handling and positioning principles used for common industrial objects cannot be easily miniaturized because of the scaling effect. In fact, the behavior of the micro-objects is highly different from the macroscale because it mainly depends on surface forces. Current industrial handling methods are consequently not adapted to this particular behavior. Several microhandling strategies have been proposed in the literature, but their current reliabilities must be improved. One way to increase the reliability of microhandling tasks consists in micromanipulate the object in a liquid [1,2]. Submerged two-fingered grippers have been proposed

*This work was supported by the French National Agency (ANR) under NANOROL contract ANR-07-ROBO-0003: Nanoanalyse for micromanipulate. The authors would like to thank also the BRIC (ULB) and the WBI-FNRS for their financial support.

†C. Lenders and P. Lambert are with Bio Electro and Mechanical Systems Department, Université Libre de Bruxelles (U.L.B.), Av. F.D. Roosevelt 50, 1050 Bruxelles, Belgium (e-mail: clenders@ulb.ac.be, plambert@ulb.ac.be)

‡M. Gauthier is with the FEMTO-ST Institute, UMR CNRS 6174 - UFC ENSMM UTBM, AS2M Department, 24 rue Alain Savary, 25000 Besançon, France (e-mail: michael.gauthier@femto-st.fr)

where the release of the object is controlled by dielectrophoresis [3] or chemical principle. Submerged ice gripper is also an original way to position micro-objects in a liquid [4]. These submerged handling methods do not enable compliance which is usually useful in micro-assembly. In other hand, in air, capillary gripping is able to grasp object with some compliance (see Fig. 1) and performs micro-assembly tasks [5]. In a general way, surface tension forces can be used as an efficient micro-actuation principle, since they become predominant at small dimensions.

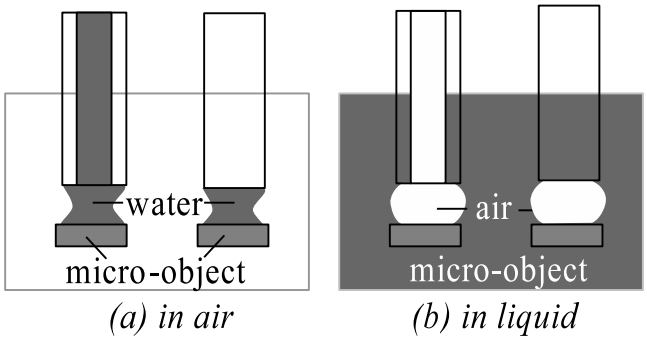

Figure 1: Principle of capillary grippers: (a) current gripper in the air, (b) frame of the paper: submerged capillary gripper

The frame of this paper deals with the study of capillary gripping in a submerged medium. To implement this principle for liquid environments, it is necessary to have a gas-liquid interface, and thus it requires generating bubbles. Consequently the first step of the study of submerged capillary handling consists in the study of the generation of single bubbles. This paper presents a model and experimentation of the bubble generation.

Some authors have already used bubbles in microsystems. For example, [6] use a bubble as a valve in a microfluidic system, and [7] propose to use bubbles as actuators.

[8, 9] have studied the continuous generation of bubbles. [10, 11] proposed numerical methods to estimate the geometry of a growing bubble. Many of these authors are interested in the size of bubbles as function of parameters such as the fluid flow at the bubble generation point. The applications of these studies are most often in the field of chemistry and colloids.

In this article, we propose a method to generate only one bubble of a defined size in a liquid. The idea is very simple: we propose to push gas to an output channel by mean of a syringe system. It offers several advantages: the gas injected is independent of the fluid, contrary to hydrolysis, and parameters are easy to control compared to the study of droplet. One of the novelty of the study of bubbles is that their behavior depends on a coupling effect between surface tension and gas compressibility.

We present in section 2 the mathematical model used to predict the shape of the bubble. The resolution of the model is presented in section 3 and will show in some cases the existence of an instability during bubble growth. We propose in section 4 a

study of dimensionless numbers, which lead to a criterion characterizing the existence of the instability. Finally, we describe in section 5 the experimental set up built to validate the model, and we present some results showing the good correspondence between the model and the experiment.

2 Bubble Growth Modeling

In this section, we present the model used to predict the generation of a gas bubble using a syringe pump. We first introduce the parameters, then the governing equations.

2.1 Parameters of the Model

The device consists of a gas tank (the syringe) and an exhaust channel (the needle) immersed in a liquid. The shape of the bubble is supposed to be a spherical cap. This means that the pressure inside the bubble is assumed to be uniform, i.e. we neglect the hydrostatic pressure due to gravity and dynamical effects, since this is an equilibrium model. The needle we used have diameters s ranging from 2 mm to 150 µm.

The parameters are shown in Table 1, and the device is illustrate on Fig. 2.

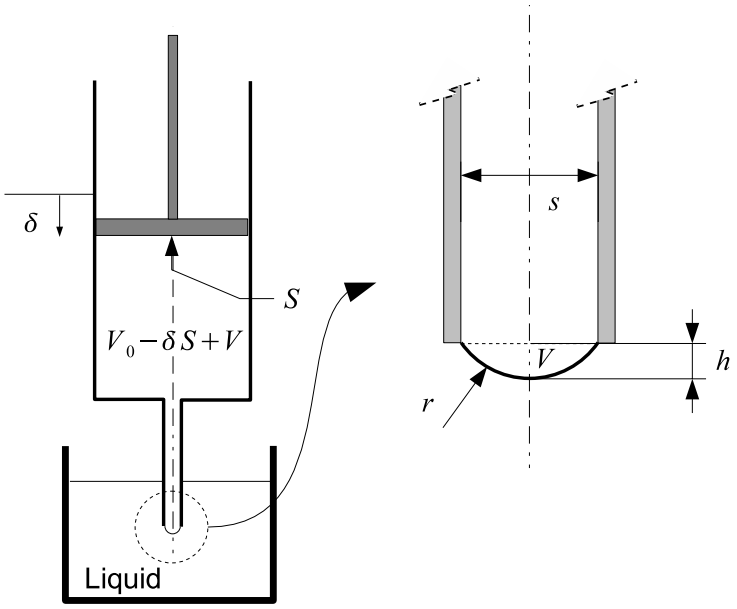

Figure 2: Schematic diagram of the bubble and the syringe

The contact angle at the edge of the outlet channel is assumed to be variable, ranging from 0° to 180°, and the contact line is assumed to stay on the inner diameter of the exhaust channel.

Table 1: Definition of model parameters

Parameter	Description
V_0 (m^3)	Initial volume in the syringe
V (m^3)	Volume of gas in the spherical cap
δ (m)	Displacement of the piston
γ ($N\,m^{-1}$)	Surface tension at the liquid-gas interface
P_0 ($N\,m^{-2}$)	Atmospheric pressure
P ($N\,m^{-2}$)	Pressure in the gas tank
T (K)	Temperature of the system
R ($N\,m\,mol^{-1}\,K^{-1}$)	Universal gas constant
n (mol)	Total number of gas mole in the system
S (m^2)	Section of the piston
s (m)	Exhaust channel diameter
r (m)	Radius of the spherical cap
h (m)	Height of the spherical cap

2.2 Governing Equations

We will build here the mathematical model of the system. The goal is to find the geometry of the bubble (defined by the height h and the radius r of the spherical cap, and the needle channel diameter s) as a function of the other parameters. The total amount of moles n in the gas is assumed to be constant.

Since the surface tension in the spherical cap will induce across its interface a pressure gradient which depends on the size of the cap, the total volume of the gas is not constant.

The pressure P in the gas phase is supposed to be uniform in the entire system.

To build the governing equation, we use three mathematical relations: Laplace equation (1), the ideal gas law (2) and the equations describing the geometry of a spherical cap (3 and 4):

$$\frac{2\gamma}{r} = P - P_0 \tag{1}$$

$$P(V + V_0 - \delta S) = nRT \tag{2}$$

$$r = \frac{s^2}{8h} + \frac{h}{2} \tag{3}$$

$$V = \frac{\pi h}{6}\left(\frac{3s^2}{4} + h^2\right) \tag{4}$$

Laplace equation (1) links the pressure gradient $P - P_0$ across the gas-liquid interface with the mean curvature $2/r$ of this interface, and the surface tension γ. The ideal gas law (2) is used to take the compressibility of the gas in account. Finally, assuming

the geometry of the interface to be a spherical cap (3,4) allows to find a relation between the tip diameter, the curvature radius and the height of the bubble. In this model, we will assume that the number of mole n is fixed by V_0 and P_0 using the ideal gas relation. This means that the syringe is filled under atmospheric pressure.

The geometry of the bubble may be defined by two of the three variables r, s and h. Since s is set by the experimental setup, we will take it as one of the parameter. We will use h as the second parameter since it allows to set the resulting equation in a polynomial form.

Hence our governing equation will be in the form $h = \mathrm{f}(V_0, P_0, \gamma, T, R, n, S, s, \delta)$. The solutions of this equation give the possible heights of the bubble.

$$\begin{aligned}
&\frac{\pi}{12}P_0h^5 + \frac{\pi}{3}\gamma h^4 + \frac{\pi}{12}P_0s^2h^3 \\
&+ \left[-\frac{1}{2}nRT + \frac{1}{2}P_0(V_0 - \delta S) + \frac{\pi}{4}\gamma s^2\right]h^2 \\
&+ \left[\frac{\pi}{64}P_0s^4 + 2\gamma(V_0 - \delta S)\right]h \\
&+ \frac{1}{8}P_0s^2(V_0 - \delta S) - \frac{1}{8}nRTs^2 = 0
\end{aligned} \tag{5}$$

This equation is a fifth order polynomial with h as dependent variable. We cannot find analytical solution, but it can be easily solved using numerical methods. This expression will potentially give one, three or five real solutions.

3 Resolution of the Model

In this section, we will solve (5) for two different sets of parameters and interpret the results. The liquid in which we create the bubble is supposed to be water and the gas is supposed to be air. Some of the parameters are common for both sets: atmospheric pressure $P_0 = 101325\,\mathrm{Pa}$, temperature $T = 298.15\,\mathrm{K}$ and surface tension $\gamma = 72 \times 10^{-3}\,\mathrm{N\,m^{-1}}$. The universal gas constant is $R = 8.314\,\mathrm{N\,m\,mol^{-1}\,K^{-1}}$.

Two different kind of behavior are obtained: the bubble is growing continuously or not, as illustrated below.

3.1 First Behavior: Continuous Growth

Let us consider a first set of parameters (Table 2).

Calculating the roots of the polynomial for each value of piston displacement δ gives the curve illustrated on Fig. 3. The dashed curve represents the height of a spherical cap having a volume $S\delta$, i.e. an incompressible fluid behavior. This clearly shows the importance of coupling between the surface tension and the compressibility of the gas on the bubble behavior. Consequently, for small piston displacement δ, the height of the bubble h is defined by a physical equilibrium between the compressibility of gas and the capillary pressure.

Table 2: Sets of parameters for model interpretation

Parameters	First set	Second set	Units
V_0	2×10^{-6}	5×10^{-9}	(m^3)
n	8.1748×10^{-5}	2.044×10^{-7}	(mol)
S	7.8540×10^{-5}	1.9635×10^{-7}	(m^2)
s	2×10^{-3}	150×10^{-6}	(m)
δ	$0 \rightarrow 25.5 \times 10^{-3}$	$0 \rightarrow 25.5 \times 10^{-3}$	(m)

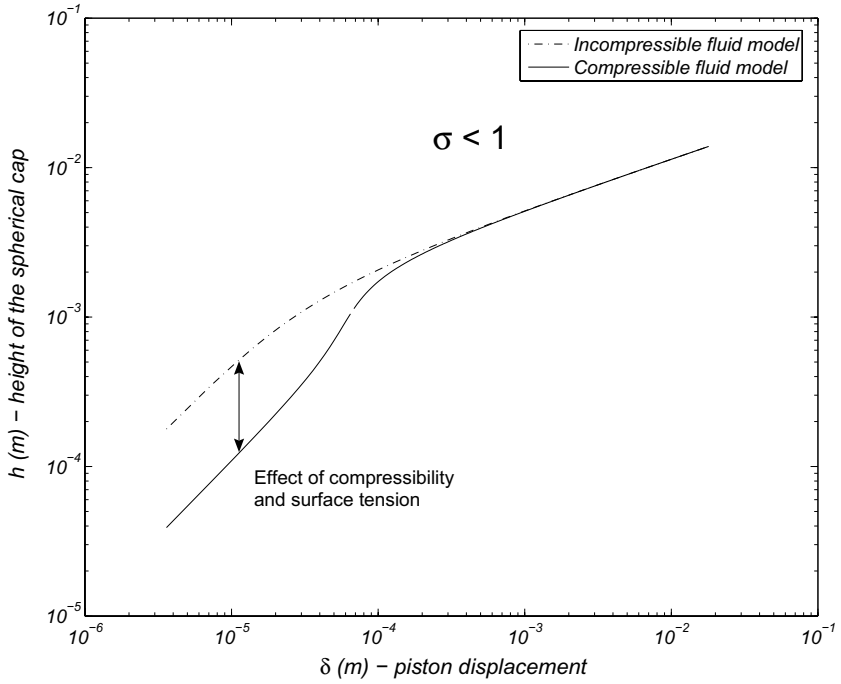

Figure 3: Simulation of bubble height h as a function of piston displacement δ, with first set of parameter. The dashed curve represents the height of a spherical cap having a volume of $S\delta$, i.e. without taking compressibility and surface tension in account. The plain curve takes compressibility and surface tension in account. One should notice the growth of the bubble is continuous

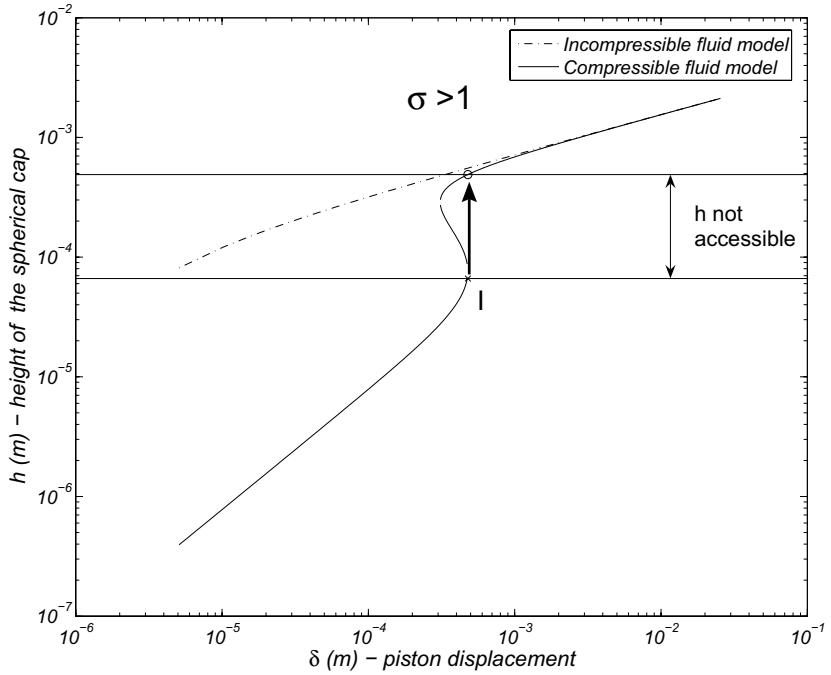

Figure 4: Simulation of bubble height h as a function of piston displacement δ, with a second set of parameter. The dashed curve represents the height of a spherical cap having a volume of $S\delta$, i.e. without taking compressibility and surface tension in account. The growth of the bubble is not continuous: the arrow illustrates the sudden transition of its height at the inflection point I. Because of this instability, there is a range of bubble height that is not accessible

From this figure, we may conclude that if we increase piston displacement δ, the height of the spherical cap will increase continuously. In this simulation, we assume that the bubble never lifts off. However, when the bubble is large enough, it will actually separate from the output channel and lift off, due to the Archimedes force.

3.2 Second Behavior: Discontinuous Growth

Let us now consider a second set of parameters (Table 2). When we plot the evolution of bubble height h as a function of piston displacement δ, we see the curve is "S"-shaped (see Fig. 4).

The consequence is that when we push the piston of the syringe (i.e. we increase δ), there is an inflection point I where a discontinuity appears. The size of the bubble will increase suddenly (arrow on Fig. 4). At this point, the bubble rapidly expands and the volume of the bubble increases rapidly (Fig. 5).

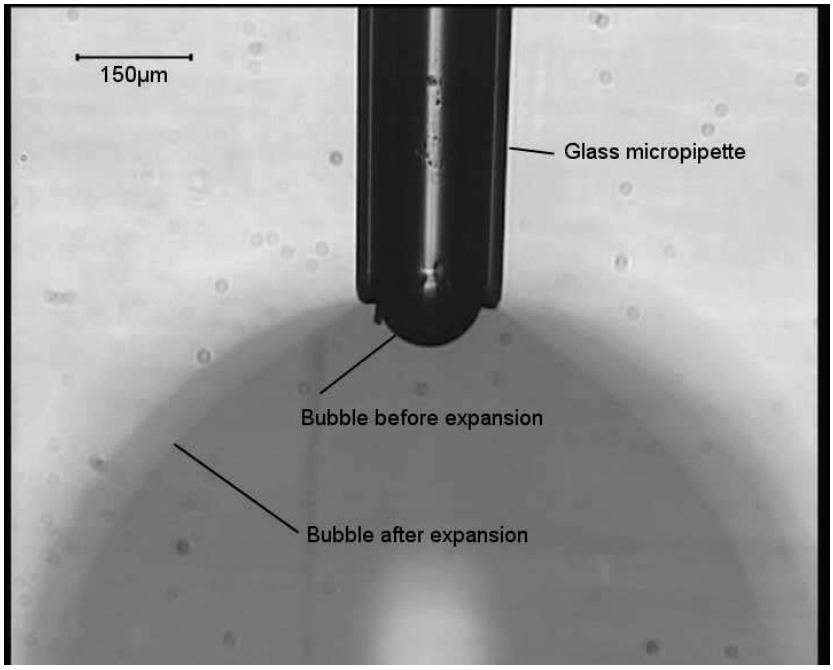

Figure 5: View of a bubble growth instability. The image has been recorded at 25fps on a CCD camera. The CCD sensor has captured in the same frame the geometry of the bubble before and after its expansion (left and right of point I on Fig. 4). The image shows the end of the glass tip used as outlet channel, the bubble generated (the half-sphere at the end of the tip), and the bubble after its sudden expansion (the shadow). This indicates that the expansion is a fast phenomenon

This instability occurs when, in our polynomial model, there are three real roots instead of one.

We observe that the maximal height before the instability occurs is close to $s/2$, i.e. a half sphere. This configuration is particular because the interface curvature is minimal, which correspond to a maximal pressure inside the bubble.

Because of this instability, there is a range of h that is not accessible. Moreover, the increase of bubble volume lead to its uncontrolled lift off.

We will propose a criterion in the next section to predict the existence of this instability.

4 Dimensionless Study

Dimensionless numbers are often used to make a similarity study on a system, or to reduce the number of parameters in a model. In this section, we use dimensionless numbers and (5) to predict whether the parameters of the system will lead to an instability or not.

The idea is to find relevant dimensionless numbers for this problem, in order to define a criterion which characterizes the stability of the bubble growth.

4.1 Dimensionless Equation

In order to find the relevant dimensionless number, we could build the dimensional matrix for each parameters, and use Buckingham theorem to find a set of dimensionless numbers [12]. However, Buckingham theorem does not provide the most relevant set of dimensionless numbers. In fact, any combination of these numbers is also a dimensionless number.

A more efficient strategy is to set our governing equation (5) in a dimensionless form. Consequently, we normalize every parameters by a combination of s and γ.

$$\tilde{E} = \frac{nRT}{\gamma s^2} \quad \tilde{S} = \frac{S}{s^2} \quad \tilde{P} = \frac{P_0}{\gamma/s}$$
$$\tilde{H} = \frac{h}{s} \qquad \tilde{V} = \frac{V_0}{s^3} \quad \tilde{\delta} = \frac{\delta}{s}$$

The equation is then rewritten using the normalized parameters (6).

$$\begin{aligned}
&\frac{\pi}{12}\tilde{P}\tilde{H}^5 + \frac{\pi}{3}\tilde{H}^4 + \frac{\pi}{12}\tilde{P}\tilde{H}^3 \\
&+ \left[-\frac{\tilde{E}}{2} + \frac{\tilde{P}}{2}\left(\tilde{V} - \tilde{\delta}\tilde{S}\right) + \frac{\pi}{4}\right]\tilde{H}^2 \\
&+ \left[\frac{\pi}{64}\tilde{P} + 2\left(\tilde{V} - \tilde{\delta}\tilde{S}\right)\right]\tilde{H} \\
&+ \frac{\tilde{P}}{8}\left(\tilde{V} - \tilde{\delta}\tilde{S}\right) - \frac{\tilde{E}}{8} = 0
\end{aligned} \tag{6}$$

It should be noticed that h is a function of 9 parameters in (5), and $\tilde{H}$ is a function of only 5 parameters in (6). The reduction reaches[1] up to the number of dimensions in the model, four in this case.

In our case, we can even go one step further. Since the output of (6) is $\tilde{H}$, it can be rewritten as follow:

$$\tilde{H} = \tilde{\mathrm{f}}\left(\tilde{P}, \tilde{E}, \tilde{V} - \tilde{\delta}\,\tilde{S}\right) \tag{7}$$

The parameters have been grouped in only 3 sets of parameters: $\tilde{E}$, $\tilde{P}$ and $\tilde{V} - \tilde{\delta}\,\tilde{S}$. Since piston displacement δ appears in the set of parameters $\tilde{V} - \tilde{\delta}\,\tilde{S}$, this set cannot influence the shape of the curve $h(\delta)$ on Fig. 3 or Fig. 4.

Consequently, it cannot influence the existence of the instability.

We can conclude that the existence of an instability when generating a bubble from a syringe pump device is only determined by two dimensionless numbers: $\tilde{E}$ and $\tilde{P}$.

4.2 Determining Threshold of the Dimensionless Numbers

Since only two dimensionless numbers should define the existence of an instability, we have run a set of numerical simulations to determine the threshold values for these dimensionless numbers beyond which the system will be unstable.

The plot in Fig. 6 shows the results of the simulations. The crosses correspond to a set of parameters that led to an instability, and the dots where no instability has been observed. There is a clear borderline between the area of instability and the area of stability. The equation of the borderline allows to define the threshold for the two dimensionless parameters.

The equation of the borderline is well approached by (8) (the line in Fig. 6).

$$\log\tilde{E} = 2\log\tilde{P} \tag{8}$$

Hence, the stability condition of the experimental setup is

$$\tilde{E} < \tilde{P}^2 \tag{9}$$

This condition can also be stated in terms of parameters with dimension:

$$\sigma = \frac{V_0\,\gamma}{P_0\,s^4} < 1 \tag{10}$$

This simple criteria characterizes the fact that the complex equation (5) has only one solution for each value of piston displacement δ, and thus that the growth of the bubble is stable. This relation can be used to plot a chart in specific conditions, in order to ease the choice of the admissible initial volume V_0 regarding the diameter of the output channel s. We have plotted this chart for a standard pressure and different values of surface tension (Fig. 7).

[1] Actually, the reduction is given by the rank of the dimensional matrix

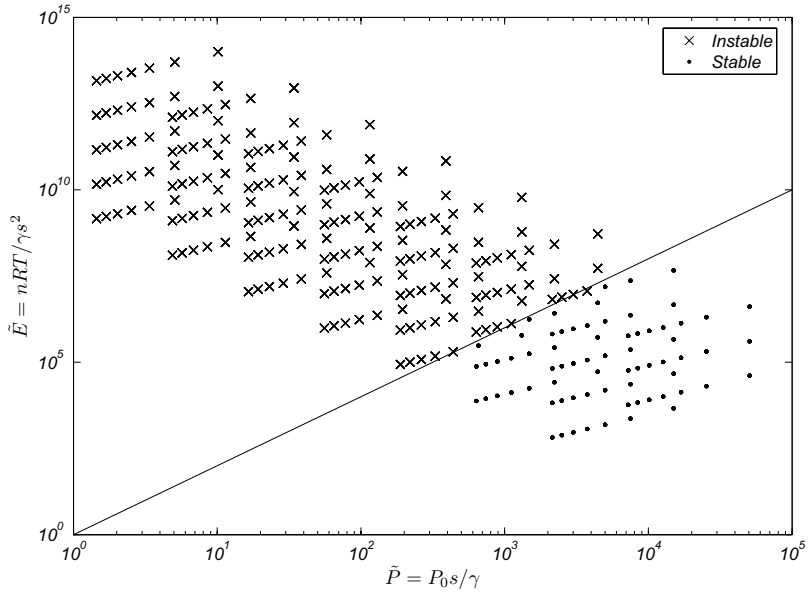

Figure 6: Search of the dimensionless number threshold. Crosses (dots) represent experimental setups that led to an instable (stable) bubble generation

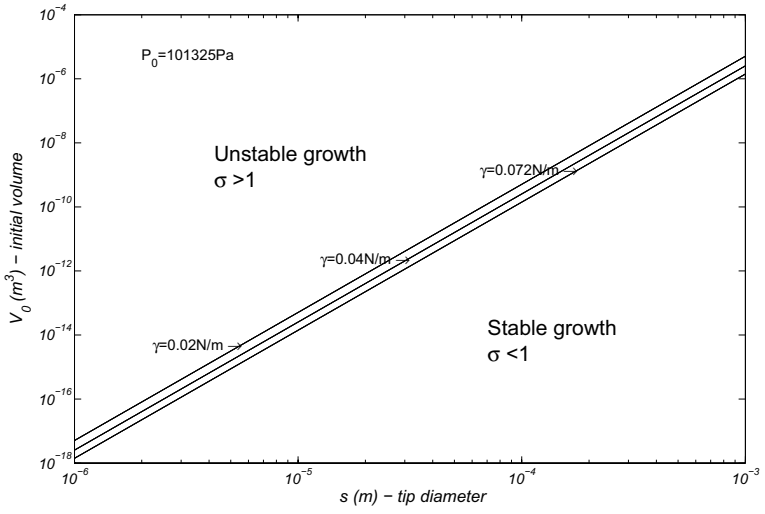

Figure 7: Chart of maximum admissible initial volume as a function of tip diameter. If V_0 is too large, the bubble generator is likely to produce unstable bubbles

4.3 Scale Effect on the Criterion

If we consider l as the typical size of the problem, the initial volume V_0 is proportional to l^3, and s is proportional to l. The stability criteria σ is thus proportional to l^{-1}. Consequently, a miniaturization induces an increase of σ and can lead a non-continuous growing.

Let us consider the case where the tip diameter is identical to the piston diameter, and let L be the maximum height of gas in the syringe. The volume is $V_0 = L\pi s^2/4$. Hence we can calculate the ratio of L as a function of a ratio of s: $(L_1/L_2) = (s_1/s_2)^2$. If the diameter of the channel is reduced by a factor of 10, the maximum height of gas in the syringe is reduced by a factor of 100.

The non-continuous growth of bubble is therefore specific to microsystems.

5 Experimental Validation

To validate the mathematical model presented here, a set of experiments has been performed to correlate the growth of a bubble with the displacement of a piston in a syringe pump device.

5.1 Experimental Bench Description

The test bench (Fig. 8) mainly consists of:

- A syringe pump, composed of a syringe whose piston is actuated by a manual microtranslation stage;
- a glass micropipette, constituting the output channel. This kind of micropipette is normally used in in vitro fertilization;
- a visualization device (including a camera), to perform the image analysis and find the height of the bubble.

The experiments are performed in DI water, and the gas injected is air.

Since the microtranslation stage is manual, we perform a quasi-static experiment by moving regularly the stage by a predefined quantity.

The images of the movie are analyzed using an edge detection function. The conversion from pixel to length is done by first calibrating the visualization device.

5.2 First Set of Experiments

The parameters for this experiment are given in Table 3.

We made two series of measurements on the same micropipette, that are compared to the theoretical value (Fig. 9). In this configuration, the dimensionless number $\sigma = 67$, agreeing with the fact that the bubble growth is not continuous.

The theoretical curve fits the general shape of the experimental curves $h(\delta)$ in good approximation. However, we observe an horizontal offset that is due to the imprecise measurement of the zero height of the spherical cap, when starting the experiment.

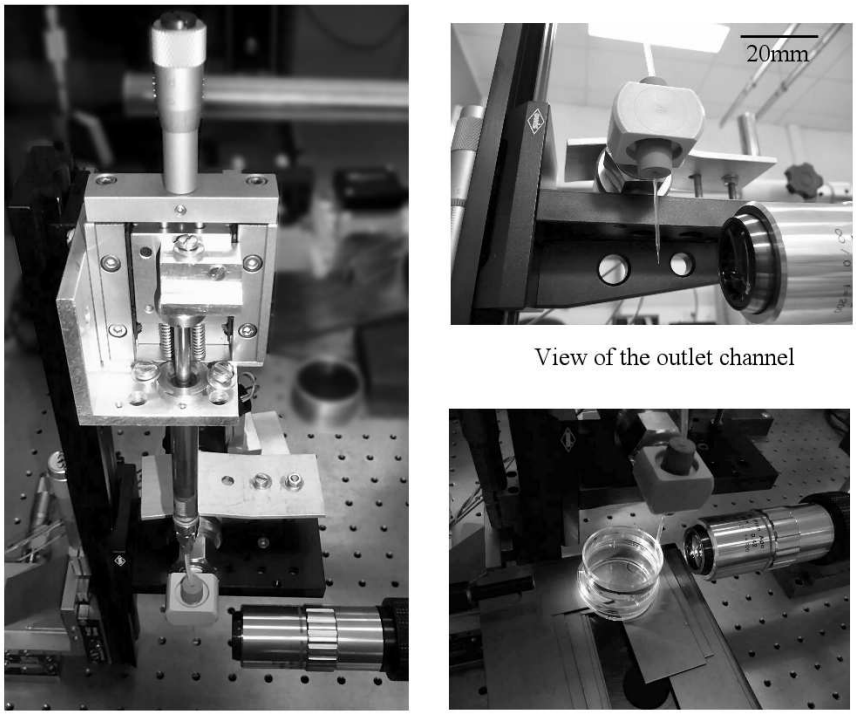

Figure 8: View of the validation test bench

Table 3: First experiment parameters

Parameters	Value
V_0	$47.65 \times 10^{-9}\,\mathrm{m}^3$ (estimation including connections)
T	between 298 K and 308 K (for theoretical curve, 298 K)
S	$9.62 \times 10^{-8}\,\mathrm{m}^2$
s	$150 \times 10^{-6}\,\mathrm{m}$

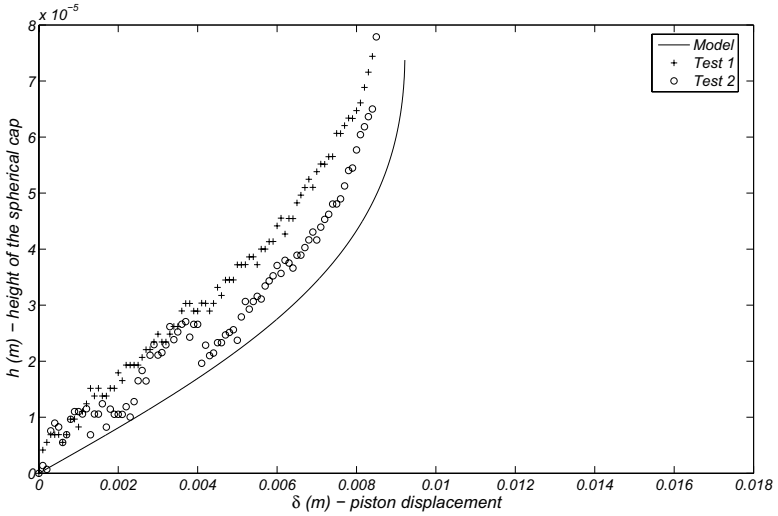

Figure 9: Experimental validation of the syringe pump bubble generator - First set of results. There is an horizontal offset because the height of the spherical cap is not zero when the experiment is started. The experiment is stopped when the bubble expands

Table 4: Second experiment parameters

Parameters	Value
V_0	$557.6 \times 10^{-9}\text{m}^3$ (estimation including connections)
T	between 298 K and 308 K (for theoretical curve, 298 K)
S	$1.96 \times 10^{-5}\text{m}^2$
s	$150 \times 10^{-6}\text{m}$

5.3 Second Set of Experiments

We performed a second set of experiments with a different syringe. The parameters are shown in Table 4. In this configuration, $\sigma = 783$.

The results of this set of experiments is shown in Fig. 10. The theoretical curve seems more steep than the trend of the experimental points. However, this can be explained by errors in the theoretical parameters. The dashed curve represent the model with a variation of 10% of its parameters (S, s, P_0 are reduced by 10% and V_0 is increased by 10%). Since the experimental points are located between the two curves, they are in agreement with the theoretical model.

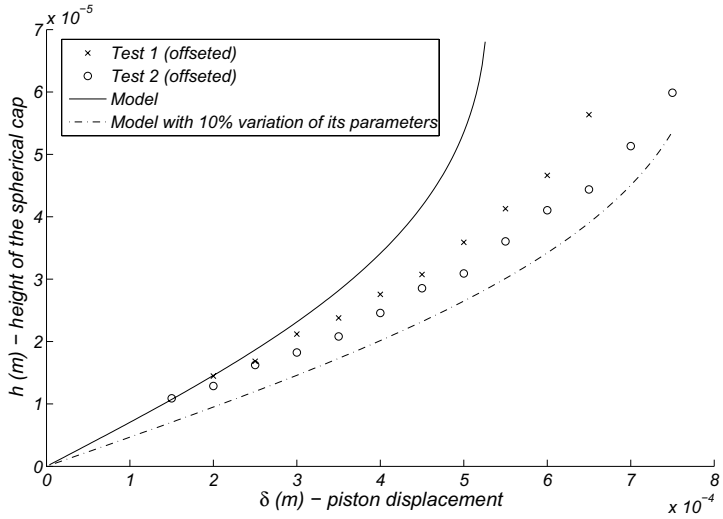

Figure 10: Experimental validation of the syringe pump bubble generator - Second set of results. The model (plain curve) do not fit the experimental points very well. However, this can be explained by errors in the parameters of the model. The dashed curve represent the model with a variation of 10% of the parameters (S, s, P_0 are reduced by 10% and V_0 is increased by 10%). The experimental points are located between the two curves, validating the model

6 Conclusions and Future Works

We have shown that controlling the generation of a bubble at microscale must be done taking into account the coupling between gas compressibility and surface tension . The developed model shows the existence of an instability under some circumstances, making the growth of the bubble discontinuous. Based on a dimensionless study of this model, a dimensionless number has been found that allows to predict the stable or unstable behavior of the system. Hence it is possible to find a threshold to design the bubble generator without instability. Finally, we have presented some experimental results to validate our model. The experimental results showed good agreement with the theoretical predictions. In micromanipulation application, this model is able to predict the growth of the bubble before the handling of the micro-object.

Future works will focus on the study of the interaction between the bubble and the grasped micro-objects. Model will be improved to take into account the micro-object. Thus the generation of microbubble proposed in this paper will be applicable to microhandling tasks based capillary forces.

References

[1] M. Gauthier, S. Régnier, P. Rougeot, and N. Chaillet, "Analysis of forces for micromanipulations in dry an liquid media," *Journal of Micromechatronics*, vol. 3, pp. 389–413, 2006.

[2] J. Dejeu, P. Rougeot, M. Gauthier, and W. Boireau, "Reduction of micro-object's adhesion using chemical functionnalisation," 2009, accepted in Micro Nano Lett., feb. 2009.

[3] M. Gauthier, E. Gibeau, and D. Hériban, "Submerged robotic micromanipulation and dielectrophoretic micro-object release," in *Proc. of the IEEE ICARCV 2006 conference, Singapore*, 2006.

[4] B. Lopez-Walle, M. Gauthier, and N. Chaillet, "Principle of a submerged freeze gripper for micro-assembly," *IEEE transactions on robotics*, vol. 24, no. 4, pp. 897–902, august 2008.

[5] P. Lambert, *Capillary Forces in Microassembly: Modeling, Simulation, Experiments, and Case Study*, ser. Microtechnology and MEMS. Springer, October 2007.

[6] H. Suzuki and R. Yoneyama, "Integrated microfluidics system with electrochemically actuated on-chip pumps and valves," *Sensors and Actuators B*, vol. 96, pp. 38–45, 2003.

[7] H. J. Lee, Y. S. Changa, Y. P. Lee, K.-H. Jeong, and H.-Y. Kim, "Deflection of microcantilever by growing vapor bubble," *Sensors and Actuators A*, vol. 136, pp. 717–722, 2007.

[8] R. B. H. Tan, W. B. Chen, and K. H. Tan, "A non-spherical model for bubble formation with liquid cross-flow," *Chem. Eng. Sci.*, vol. 55, pp. 6259–6267, 2000.

[9] H. K. Nahra and Y. Kamotani, "Prediction of bubble diameter at detachment from a wall orifice in liquid cross-flow under reduced and normal gravity conditions," *Chem. Eng. Sci.*, vol. 58, pp. 55–69, 2003.

[10] Z. Xiao and R. B. Tan, "An improved model for bubble formation using the boundary-integral method," *Chem. Eng. Sci.*, vol. 60, pp. 179–186, 2005.

[11] Z. Yang, T. Dinh, R. Nourgaliev, and B. Sehgal, "Numerical investigation of bubble growth and detachment by the lattice-boltzmann method," *International Journal of Heat and Mass Transfer*, vol. 44, pp. 195–206, 2001.

[12] T. Szirtes, *Applied Dimensional Analysis and Modeling*. New York: MacGraw-Hill, 1997.